



# Fluorescence lifetime imaging with a low-repetition-rate passively mode-locked diode-pumped Nd:YVO<sub>4</sub> oscillator

Sandrine Leveque-Fort, Dimitris N. Papadopoulos, Sébastien Forget, François Balembois, Patrick Georges

## ► To cite this version:

Sandrine Leveque-Fort, Dimitris N. Papadopoulos, Sébastien Forget, François Balembois, Patrick Georges. Fluorescence lifetime imaging with a low-repetition-rate passively mode-locked diode-pumped Nd:YVO<sub>4</sub> oscillator. *Optics Letters*, 2005, 30 (2), pp.168-170. hal-00700746

**HAL Id: hal-00700746**

**<https://hal-iogs.archives-ouvertes.fr/hal-00700746>**

Submitted on 23 May 2012

**HAL** is a multi-disciplinary open access archive for the deposit and dissemination of scientific research documents, whether they are published or not. The documents may come from teaching and research institutions in France or abroad, or from public or private research centers.

L'archive ouverte pluridisciplinaire **HAL**, est destinée au dépôt et à la diffusion de documents scientifiques de niveau recherche, publiés ou non, émanant des établissements d'enseignement et de recherche français ou étrangers, des laboratoires publics ou privés.

# Fluorescence lifetime imaging with a low-repetition-rate passively mode-locked diode-pumped Nd:YVO<sub>4</sub> oscillator

S. Lévêque-Fort

*Laboratoire de Photophysique Moléculaire, Centre National de la Recherche Scientifique, Unité Propre de Recherche 3361, Centre Universitaire, Bâtiment 210, Orsay 91405, France*

D. N. Papadopoulos, S. Forget, F. Balembois, and P. Georges

*Laboratoire Charles Fabry de l'Institut d'Optique, Centre National de la Recherche Scientifique, et Université Paris Sud, Unité Mixte de Recherche 8501, Centre Universitaire, Bâtiment 503, Orsay 91403, France*

Received August 18, 2004

We report a wide-field fluorescence lifetime imaging microscope based on a low-repetition-rate (3.7-MHz) passively mode-locked diode-pumped laser source. This inexpensive and compact laser source operating in the visible and UV range can excite a wide range of fluorophores of biological interest. We demonstrate that the power of this laser source is highly sufficient for studying biological systems with low quantum yields (autofluorescence of tissues and stained living cells). The maximum measurable lifetime is also strongly increased with this laser source, as fluorescence intensity measurement can occur 250 ns after the excitation pulse.

© 2005 Optical Society of America

OCIS codes: 140.3480, 140.4050, 170.2520, 170.3650.

Fluorescence lifetime is a powerful spectroscopic tool, as it is not only sensitive to the type of fluorophore but also depends on its local environment [e.g., ion concentrations, polarity, pH (Ref. 1)]. Independent of fluorophore concentration, fluorescence lifetime measurements are thus a robust approach to extracting probes with a low fluorescence quantum yield and, in addition, can be used to distinguish fluorophores with overlapping emission spectra. Fluorescence lifetime imaging (FLIM) provides maps of the spatial distribution of the fluorescence lifetime, adding a powerful functional imaging approach for biomedical investigations. FLIM has been demonstrated both in the frequency domain by use of modulated cw lasers and in the time domain by use of ultrashort pulsed lasers. Although the frequency domain is more commonly used because it appears more straightforward and cheaper<sup>2,3</sup> to implement for monoexponential decay with nanosecond decay time, the time domain is much more suitable for extracting multiexponential decay and reaching picosecond resolution. Recent advances in ultrafast gated optical intensifiers and in ultrafast laser sources have opened up new opportunities for time-resolved fluorescence microscopy. In the time domain the maximum measurable lifetime depends strongly on the repetition rate of the laser system. To perform a proper analysis of the fluorescence decay, it is strongly recommended that the biological system be allowed to relax during at least three times the fluorescence lifetime before sending a new pulse. As most setups are based on commercial Ti:sapphire (~80 MHz), they are limited to a lifetime of less than 4 ns, and the longest lifetime can be measured only by use of a pulse picker or a cavity dumper, thus adding extra cost and complexity. A pulsed diode was recently proposed<sup>4</sup> as an alternative to this approach, but it offers a much lower excitation power and could present a postpulse that is not suitable

for FLIM measurement. In this Letter we present a time-domain FLIM microscope based on a home-built diode-pumped picosecond laser source working at 3.7 MHz that allows one to strongly increase the range of measurable lifetimes to 80 ns. By frequency doubling and tripling the laser, excitation at either 355 or 532 nm can be easily produced with an average power of several tens of milliwatts. These two excitation wavelengths allow us to cover a wide range of intrinsic fluorophores and commonly used biological fluorescent probes, with an incident power far above the value typically used (1 mW).

A complete description of the laser source principle can be found elsewhere.<sup>5</sup> For mode-locked lasers, the pulse repetition frequency is directly proportional to the inverse of the cavity length:  $PRF = c/2L$ , where  $c$  is the speed of light and  $L$  is the optical length of the laser resonator. Therefore the designed cavity here is 40 m long to yield a 3.7-MHz repetition rate (a longer cavity could easily be made with the same design<sup>5</sup>). This length is obtained by use of an intracavity multipass cell that allows the laser beam to bounce ~40 times between two sets of highly reflective mirrors. To compensate for the losses introduced by these multiple reflections, we used a Nd:YVO<sub>4</sub> crystal, known for its high gain, as the gain medium. The 0.1% Nd-doped crystal is 0.5 mm long and pumped by a 15-W fiber-coupled laser diode emitting near 808 nm. Passive mode locking is achieved with a semiconductor saturable absorber. With this setup, 16-ps-long pulses are produced in a diffraction-limited beam, and the average output power is ~1 W at 1064 nm. Second- or third-harmonic generation can then be performed in KTP and  $\beta$ -barium borate crystals, respectively, leading to several tens of milliwatts at 532 or 355 nm for direct excitation of the sample. Epifluorescence imaging was carried out at room temperature with a home-built inverted microscope

(Fig. 1). To excite the sample with Kohler illumination, the laser beam is first expanded and collimated, then focused onto the back focal plane of the objective [Apochromat, Zeiss, 63 $\times$ , numerical aperture (NA) of 1.4, oil immersion]. Wide-field fluorescence images ( $100\text{ }\mu\text{m} \times 120\text{ }\mu\text{m}$ ) are acquired at very low excitation light levels (less than 1 mW). The fluorescence collected by the microscope objective is separated from any reflected excitation light by a dichroic beam splitter and an interference filter before being imaged onto a high-rate imager (HRI, Kentech Instruments). The HRI produces a time-gated fluorescence intensity image at a repetition rate of 3.7 MHz with a gate width ranging from 200 ps to 1 ns. The images from the HRI are optically relayed to a 12-bit CCD camera (Hamamatsu Orca ER, binning  $2 \times 2$ ). By use of a programmable delay generator, time-gated intensity images are acquired at different delays after the excitation pulse. FLIM maps are thus produced by recording a series of 2–30 time-gated fluorescence intensity images and fitting the data for each image pixel to a single exponential decay model by use of a standard nonlinear least-squares fitting algorithm. Intensity images are obtained by adding the series of time-gated intensity images.

By using the laser at either 355 or 532 nm, one can obtain a FLIM map of biological samples by exciting their autofluorescence. Two different samples are presented in Fig. 2: a fixed section of prostate tissue and an urothelial cell. Figures 2(a) and 2(d) show the white-light transmission image; Figs. 2(b) and 2(e) and 2(c) and 2(f) show the corresponding fluorescence intensity and lifetime image, respectively. The prostate tissue was imaged with the laser at 355 nm. The fluorescence intensity image [Fig. 2(b)] allows us to identify the different structures inside a thin section of tissue, and we can thus clearly see that the nucleus presents a lower fluorescence intensity. The corresponding FLIM map [Fig. 2(c)] exhibits a complementary contrast with a short lifetime (300–950 ps). The urothelial cell was excited at 532 nm, and the fluorescence was spectrally filtered (550-nm peak wavelength, 50-nm width) to remove the strong fluorescence from the background. On the fluorescence intensity image [Fig. 2(e)] we can clearly distinguish the nucleus that presents a lower intensity. This difference of intensity is due only to a difference in the concentrations of the fluorophores as in the FLIM image [Fig. 2(f)]; the whole cell presents a homogeneous lifetime with an average value of 2.9 ns (0.16-ns standard deviation). These results demonstrate that the laser is thus highly suitable for taking advantage of autofluorescence of biological samples but can also be used to excite a wide range of dyes or probes that absorb in the UV–visible range. The second main advance offered by the new laser source for FLIM is the optimal delay between two excitation pulses, which allows one to properly measure lifetime. FLIM maps of stained living cells were obtained by use of the doubled frequency of the laser source (532 nm). HeLa cells grown on glass coverslips were incubated with 12  $\mu\text{g}/\text{ml}$  of ethidium bromide in a growth

medium for 30 min at 37 °C. Ethidium bromide is a well-known DNA-specific fluorochrome that presents a short lifetime in its free state (1.8 ns) and should exhibit strong fluorescence enhancement and a longer lifetime (22 ns) when intercalated in the nucleus of living cells.<sup>6,7</sup> Figure 3(a) shows a typical result with fluorescence intensity images of three cells, where a strong fluorescence due to ethidium–DNA binding is observed inside the cells as expected. To calculate the FLIM map, 23 time-gated fluorescence intensity images were recorded up to 120 ns after the excitation pulse. Three time-gated intensity images taken along the fluorescence decay are shown in Figs. 3(d), 3(e), and 3(f) and correspond to time delays after excitation pulses of 300 ps, 45 ns, and 80 ns. The corresponding FLIM map [Fig. 3(c)] process with a single

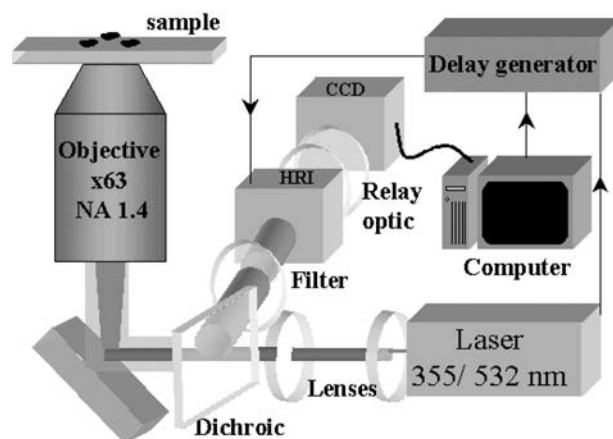


Fig. 1. Experimental setup for wide-field fluorescence microscopy.

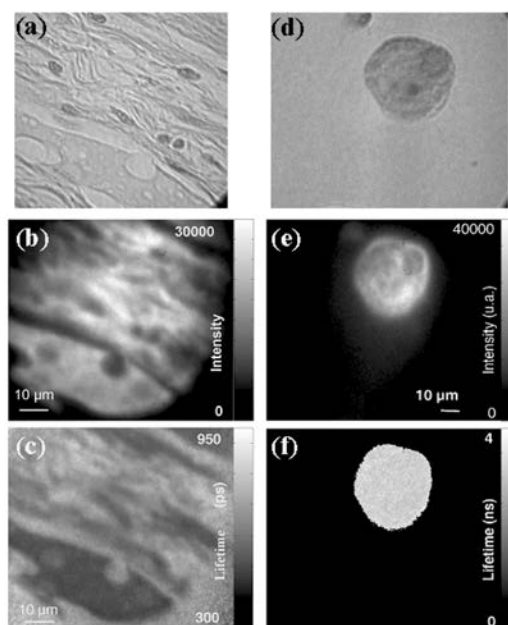


Fig. 2. (a)–(c) Fixed prostate tissue investigated under 355 nm; (d)–(f) urothelial cell with the laser at 532 nm and a filter at the detection point (centered at a 550-nm width of 50 nm). (a), (d) Transmission images; (b), (e) fluorescence intensity images; (c), (f) fluorescence lifetime images.

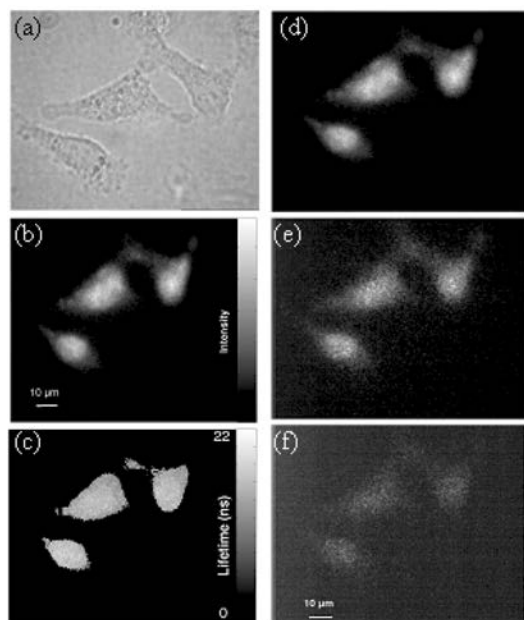


Fig. 3. (a) Transmission image of three HeLa cells grown on a coverslip and incubated with ethidium bromide. (b), (c) Corresponding intensity and FLIM image, respectively. (d), (e), (f) Time-gated intensity images taken along the fluorescence decay 300 ps, 45 ns, and 80 ns after the excitation pulse, respectively.

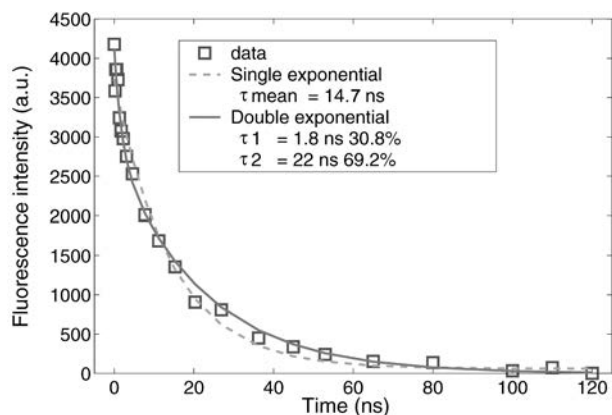


Fig. 4. Typical fluorescence decay data inside a cell fitted with a single and a double exponential model.

exponential model clearly exhibits good uniformity with a mean lifetime of 14.7 ns. On a fluorescence decay extracted from one pixel inside a cell, we performed a fitting routine with a single and double exponential decay (Fig. 4). The plots confirm that the single exponential model is a quick way to obtain a FLIM map exhibiting a mean value for the lifetime, but the fitting failed for the first data points and tends to overestimate the last ones. A double exponential model is thus more appropriate in this case (reduction

of the chi square by a factor of 7), and we clearly see the presence of two states of the ethidium: a free state with  $\tau_1 = 1.8$  ns and a weight of 30.8% and an intercalated state with  $\tau_2 = 22$  ns and a weight of 69.2% of the fluorescence. We also point out the benefit of the later fluorescence measurements obtained in this case 120 ns after the excitation pulse, which leads to a more stable fit and avoids a shorter and noisier FLIM map.

In summary, we have combined a new passively mode-locked diode-pumped laser source with a wide-field microscope. We have demonstrated high suitability of this setup for biological investigations and especially for lifetime imaging, as the low repetition rate of the laser source allowed us to properly analyze the fluorescence decay. We note that this new approach should also be invaluable for several biological imaging approaches such as fluorescence anisotropy imaging of samples with a long rotational correlation time<sup>7,8</sup> or time-gated imaging based on tagging with quantum dots, in which the long lifetime of the quantum dot can be used to enhance the contrast.<sup>9</sup>

This research was partially supported by the research program Pôle Laser from the Contrat Plan Etat Région (2000–2006) (French State and Conseil Général de l'Essonne). The authors thank S. Ferlicot, who prepared tissue and urothelial cell samples. D. N. Papadopoulos worked for this project under a Marie Curie fellowship, and his present address is the Lasers and Applications Group, Department of Physics, National Technical University of Athens, Heroon Polytechniou 9, Athens 15780, Greece. S. Lévêque-Fort's e-mail address is sandrine.fort@ppm.u-psud.fr.

## References

1. R. Sanders, A. Draaijer, H. C. Gerritsen, P. M. Houpt, and Y. K. Levine, *Anal. Biochem.* **227**, 302 (1995).
2. P. T. C. So, T. French, W. M. Yu, K. M. Berland, C. Y. Dong, and E. Gratton, *Bioimaging* **3**, 49 (1995).
3. M. J. Booth and T. Wilson, *J. Microsc. (Oxford)* **214**, 36 (2003).
4. D. S. Elson, J. Siegel, S. E. D. Webb, S. Lévêque-Fort, M. J. Lever, P. M. W. French, K. Lauritsen, M. Wahl, and R. Edmann, *Opt. Lett.* **27**, 1409 (2002).
5. D. N. Papadopoulos, S. Forget, M. Delaigue, F. Druon, F. Balembois, and P. Georges, *Opt. Lett.* **28**, 1838 (2003).
6. J. Olmsted and D. R. Kearns, *Biochemistry* **16**, 3647 (1977).
7. M. Tramier, K. Kemnitz, C. Durieux, J. Coppey, P. Denjean, R. B. Pansu, and M. Coppey-Moisand, *Biophys. J.* **78**, 2614 (2000).
8. J. Siegel, K. Suhling, S. Lévêque-Fort, S. E. D. Webb, D. M. Davis, D. Philips, Y. Sabharwal, and P. M. W. French, *Rev. Sci. Instrum.* **74**, 182 (2003).
9. M. Dahan, T. Laurence, F. Pinaud, D. S. Chemla, A. P. Alivisatos, M. Sauer, and S. Weiss, *Opt. Lett.* **26**, 825 (2001).